

Krylov complexity in quantum field theory, and beyond

Alexander Avdoshkin,^a Anatoly Dymarsky,^b Michael Smolkin^c

^a*Department of Physics, MIT, Cambridge, MA 02139, USA*

^b*Department of Physics and Astronomy,
University of Kentucky,
506 Library Drive,
Lexington, KY, USA 40506*

^c*The Racah Institute of Physics, The Hebrew University of Jerusalem,
Jerusalem 91904, Israel*

ABSTRACT: We study Krylov complexity in various models of quantum field theory: free massive bosons and fermions on flat space and on spheres, holographic models, and lattice models with a UV-cutoff. In certain cases, we observe asymptotic behavior in Lanczos coefficients that extends beyond the previously observed universality. We confirm that, in all cases, the exponential growth of Krylov complexity satisfies the conjectured inequality, which generalizes the Maldacena-Shenker-Stanford bound on chaos. We discuss the temperature dependence of Lanczos coefficients and note that the relationship between the growth of Lanczos coefficients and chaos may only hold for the sufficiently late, truly asymptotic regime, governed by physics at the UV cutoff. Contrary to previous suggestions, we demonstrate scenarios in which Krylov complexity in quantum field theory behaves qualitatively differently from holographic complexity.

1 Introduction

Dynamics in Krylov space, and the associated K(rylov) complexity, have recently emerged as a new probe of the chaotic dynamics of quantum systems. Starting from an autocorrelation function $C(t)$ of a sufficiently simple, e.g. local operator A , via recursion method one can define Lanczos coefficients b_n , which control and characterize the operator growth in the Krylov subspace. The original work [1] proposed the universal operator growth hypothesis, which connects the asymptotic behavior of b_n with the type of dynamics exhibited by the underlying system. Namely, for a generic physical systems without apparent or hidden symmetries b_n will exhibit maximal possible growth consistent with locality, $b_n \propto n$ for spatially extended systems in $D > 1$. This hypothesis is essentially the quantum version of an earlier observation, that relates the high-frequency tail of the power spectrum $f^2(\omega)$ – the Fourier of $C(t)$ – with presence or lack of integrability in classical spin models [2]. Similarly, the hypothesis can be understood as a statement that in typical non-integrable lattice systems the norm of nested commutators $[H, [H, \dots A]]$, or equivalently the norm of A subject to Euclidean time evolution, grows with the maximal speed allowed by universal geometric constraints [3]. There is non-trivial evidence supporting the connection between the behavior of b_n and integrability/chaos, yet it does not seem to be universal. In particular a possible stronger formulation, relating the linear growth of b_n specifically to chaotic behavior of the underlying systems is apparently wrong [4, 5]. We observe that for continuous systems and local operator A , Lanczos coefficients always exhibit linear growth. The situation is changed if a UV-cutoff is introduced, in which case we propose the asymptotic behavior of b_n would probe integrability or lack thereof in the lattice model underlying the UV regime.

Besides being a probe of chaos, the Krylov complexity has a very intriguing and non-trivial connection with the exponent controlling the growth of the Out of Time Ordered Correlator (OTOC). Namely, the original work [1] conjectured (and proved for the case of infinite temperature) that the exponent of Krylov complexity bounds the exponent of OTOC, $\lambda_{\text{OTOC}} \leq \lambda_{\text{K}}$. We further propose this inequality being a part of a stronger relation, which generalizes the Maldacena-Shenker-Stanford bound on chaos [6],

$$\lambda_{\text{OTOC}} \leq \lambda_{\text{K}} \leq \frac{2\pi}{\beta}. \tag{1.1}$$

In most cases considered so far, the first inequality in (1.1) is non-trivial, while the second one trivially becomes an equality [3]. A proof of (1.1) in such a scenario was recently given in [7]. Below we give examples of free massive bosons and fermions,

when the first inequality is trivial (we assign $\lambda_{\text{OTOC}} = 0$ for theories not exhibiting the exponential growth of OTOC), while the second inequality becomes non-trivial. We numerically show that in this case $\lambda_K \leq \frac{2\pi}{\beta}$ is satisfied, thus providing further evidence for (1.1).

The third virtue of Krylov complexity is its potential connection to other measures of complexity in quantum systems, in particular, holographic complexity [8–14]. Earlier studies of K complexity, specifically, in the SYK model [15], suggested its qualitative behavior matches that of holographic complexity. In particular, complexity grows linearly in earlier times and then saturates at the exponential values [8, 13]. We analyze K-complexity for fields compactified on spheres and show its behavior is different from the one described above. Hence, we concluded that K complexity, despite its name, in field theories can be qualitatively very different from its computational or holographic “cousins.”¹

The connection between K complexity and open questions of quantum dynamics make it a popular subject of study [4, 5, 17–50], though with a few exceptions most of the literature is focusing on discrete models. In this paper we continue the study of K complexity in quantum field theory, initiated in [4]. There we considered only conformal field theories in flat space. Now we consider models with mass, compact spatial support and/or UV-cutoff and find rich behavior, supporting main conclusions outlined above. Interestingly, each deformation we considered – mass, compact space or UV-cutoff have their own imprint on Lanczos coefficients b_n , though universality of these imprints is unclear. Our paper sheds light on temperature dependence of b_n as well as the role of locality. It frames QFT as an IR limit of some discrete system, connecting the behavior of b_n between different limiting cases.

This paper is organized as follows. In section 2.2 we give preliminaries of Lanczos coefficients and Krylov complexity. We proceed in section 3 to consider free massive scalar and fermions to observe the effect of mass, which causes the exponent of Krylov complexity to decrease. In section 4 we compactify CFTs on a sphere to notice that this results in a capped Krylov complexity, at least in certain scenarios. Section 5 continues with the role of temperature and UV cutoff. We conclude with a discussion in section 6.

¹Krylov complexity draws its name from the fact that its definition matches certain axioms of complexity [1], but there was no strong reason to expect it would match computational or holographic complexities, which characterize the whole quantum state of the system, not merely an operator growth in Krylov space. An attempt to reconcile these discrepancies is recently taken in [16].

2 Dynamics in Krylov space and chaos

2.1 Preliminaries

The starting point to define Lanczos coefficients is a two-point function $C(t) = \langle A(t)A \rangle$ of an operator A . Once $C(t)$ is given, Lanczos coefficients b_n are related to derivatives $C^{(k)}(0)$ as explained in e.g. [17]. Assuming $C(t)$ is even,

$$b_0^2 = C''(0)/C(0), \quad b_1^2 = C^4(0)/C''(0) - C''(0)/C(0), \quad \dots \quad (2.1)$$

The tri-diagonal symmetric matrix $\mathcal{L}_{n,n} = 0$, $\mathcal{L}_{n,n+1} = b_n$ is the Liouvillian, it represents adjoint action of the Hamiltonian H in Krylov space

$$\mathcal{L}_{nm} \equiv \langle n | \text{ad}_H | m \rangle, \quad (2.2)$$

where $|n\rangle$ is the n -th normalized basis element in Krylov space. Krylov complexity is defined as

$$K(t) = \sum_{n=0}^{\infty} n |\langle 0 | e^{i\mathcal{L}t} | n \rangle|^2. \quad (2.3)$$

Mathematically, it is only a function of Lanczos coefficients b_n . While it is fully determined by $C(t)$, the relation between $C(t)$ and $K(t)$ is non-trivial.

2.2 Lanczos coefficients and chaos

All three formulations of the “signature of chaos” mentioned in the introduction: through the high-frequency behavior of the power spectrum [2]

$$f^2(\omega) = \frac{1}{2\pi} \int dt e^{i\omega t} C(t), \quad (2.4)$$

through the growth of $|A(it)|$ [3], and through the asymptotic behavior of b_n [1], are essentially mathematically equivalent, but there are some important subtleties. The exponential asymptotic

$$f^2(\omega) \sim e^{-\omega/\omega_0} \quad (2.5)$$

is equivalent to a pole of $C(t)$ at $t = i/\omega_0$, which is the same as the divergence of the Frobenius norm of $e^{-\beta H/4} A(t) e^{-\beta H/4}$ at $t = i/(2\omega_0)$, as follows from the definition

$$C(t) \propto \text{Tr}(e^{-\beta H/2} A(t) e^{-\beta H/2} A(0)). \quad (2.6)$$

This is equivalent to asymptotic linear growth

$$b_n \sim \frac{\pi}{2\omega_0} n \quad (2.7)$$

assuming asymptotically b_n is a smooth function of n . Thus (2.7) implies (2.5), but the other way around may not be true provided b_n exhibits some complicated behavior, for example b_n split into two branches for even and odd n . The reference [3] provided a mathematical example of this kind,² when b_n asymptotically split into two branches,

$$b_n^2 \sim \begin{cases} n^2, & n \text{ is even,} \\ n, & n \text{ is odd,} \end{cases} \quad (2.8)$$

while corresponding power spectrum exhibits asymptotic behavior $f^2 \propto \omega^{-\omega}$, which is an analog of (2.5) for 1D systems.³

For *any* field theory and a local operator $A(t)$ (or a local operator integrated over some region), singularity of the two-point function when the operators collide immediately implies (2.5) with $\omega_0 = 2/\beta$. Hence, trivially, the asymptotic behavior of $f^2(\omega)$ can not be used as a probe of chaos. This prompts the question if perhaps in field theory b_n may exhibit some complex behavior such that asymptotic behavior of b_n may distinguish integrability from chaos, while (2.5) would always be satisfied. A study of conformal field theories in flat space in [4] revealed that nothing of the sort happens and b_n demonstrate a “vanilla” asymptotic behavior fixed by the singularity of $C(t)$ at $t = i\beta/2$,

$$b_n = \frac{\pi}{\beta}(n + \Delta + 1/2) + o(n), \quad n \gg 1, \quad (2.9)$$

where Δ is the dimension of the operator A controlling the pole singularity at $t = i\beta/2$,

$$C(t) \sim \frac{1}{(t - i\beta/2)^{2\Delta}}. \quad (2.10)$$

Now we ask if this is perhaps a feature of conformal models in flat space that b_n always grow as $b_n \propto n$, while for more complicated QFTs Lanczos coefficients may exhibit more complex behavior. And indeed, as we see below, once scale is introduced through a mass or space volume, coefficients b_n may split into even and odd branches, with different asymptotic behavior, while (2.5) with $\omega_0 = 2/\beta$ is always satisfied.

²An example of a physical system exhibiting different power law behavior of even and odd branches of b_n is possibly given by the large- q SYK model [48].

³For 1D systems, the two-point function $C(t)$ is analytic in the entire complex plane [51]. Accordingly, the slowest possible decay of the power spectrum for large ω is, schematically, $f^2 \propto \omega^{-\omega}$. This corresponds to maximal possible growth of the norm of nested commutators $|[H, [H, \dots A]]|$ allowed by 1D geometry [3]. Corresponding maximal growth of Lanczos coefficients is $b_n \propto n/\ln(n)$ [1].

3 Free massive fields in flat space

In this section we consider free massive scalar⁴ and Dirac fermion in d spacetime dimensions, for which the correlation functions are given by, see Appendix A,

$$C(t) = \text{Tr}(e^{-\beta H/2} \phi(t, x) e^{-\beta H/2} \phi(0, x)) \propto \int_{\tilde{m}}^{\infty} (y^2 - \tilde{m}^2)^{\frac{d-3}{2}} \frac{\cosh(y\tau)}{\sinh(y/2)} dy$$

and

$$C(t) = \text{Tr}(e^{-\beta H/2} \psi^\dagger(t, x) e^{-\beta H/2} \psi(0, x)) \propto \int_{\tilde{m}}^{\infty} dy (y^2 - \tilde{m}^2)^{\frac{d-3}{2}} \frac{y \cosh(y\tau) \pm \tilde{m} \sinh(y\tau)}{\cosh(y/2)},$$

where $\tau \equiv it/\beta$, and $\tilde{m} = \beta m$. In the first case Lanczos coefficients split into even and odd branches, both growing linearly with n albeit with different intercepts, as shown for $d = 4$ in the left panel of Fig. 5.2. We call this behavior “persistent staggering”: b_n grow linearly, with the universal slope $\pi n/\beta$, but even and odd branches have different finite terms:

$$b_n = \begin{cases} \frac{\pi}{\beta}(n + c_e) + o(n), & \text{even } n, \\ \frac{\pi}{\beta}(n + c_o) + o(n), & \text{odd } n, \end{cases} \quad n \gg 1. \quad (3.1)$$

In the second case of free massless fermions $C(t)$ is not an even function, hence besides b_n , Lanczos coefficients also include a_n , see Appendix B. In this particular case coefficients $a_n = \pm(-1)^n \tilde{m}$ can be expressed analytically, while b_n exhibit standard “vanilla” asymptotic (2.9) $\beta b_n = \pi n$, see the right panel of Fig. 5.2.

Both the persistent staggering and oscillating a_n have similar effects on Krylov complexity, which we calculate in both cases numerically, see Fig. 2. Namely, $\ln K(t)$ continues to grow linearly, but with the slope λ_K smaller than $2\pi/\beta$. This provides a non-trivial test of the second inequality in (1.1). The first inequality is satisfied trivially because we assign $\lambda_{\text{OTOC}} = 0$ in free field theories.

From the mathematical point of view, it is not entirely clear which property of $C(t)$ is a cause for persistent staggering. (We are focusing on the case of even $C(t)$ here, when $a_n \equiv 0$.) Based on a handful of examples reference [52] claims, apparently erroneously, this is due to periodicity of $C(t)$. We propose that persistent staggering is a reflection of the “mass gap” of $f^2(\omega)$, that it is zero for $|\omega|$ smaller than some finite

⁴Also see [49], which similarly considered free massive scalar field and found “persistent staggering” $c_o \neq c_e$. The original version of [49] also reported different values of slopes for odd and even branches of b_n , both smaller than π/β . We regard this as a numerical artifact – we show in Appendix E that in case of two different slopes, in full generality one slope is always larger than, and the other is always smaller than π/β , see (E.33).

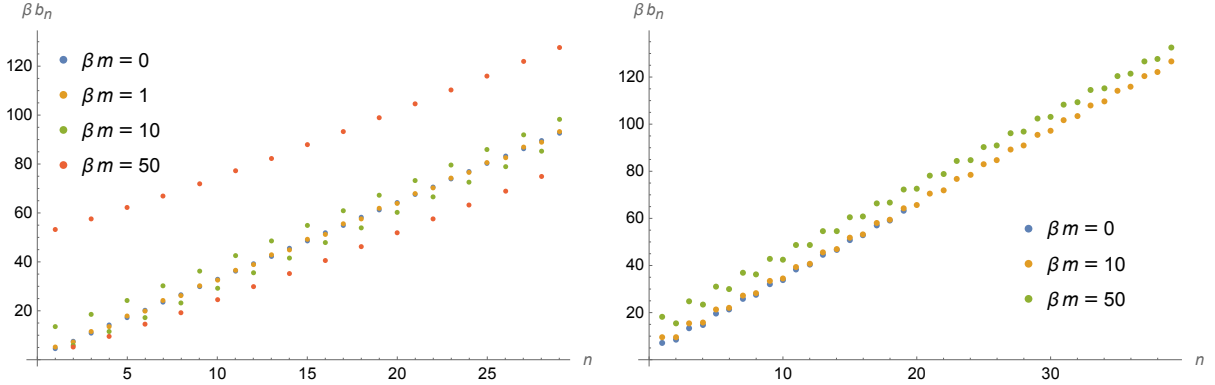


Figure 1. Lanczos coefficients for free massive scalar (left) and fermion (right) in $d = 4$ dimensions. Values for the conformal (massless) cases we discussed in [4]. For the scalar, introduction of $\tilde{m} = \beta m$ results in “persistent staggering” of b_n around the conformal values (larger \tilde{m} causes larger staggering amplitude) but does not change the slope $\pi n/\beta$. Lanczos coefficients split into two branches, see eq. 3.1. For fermions, asymptotically, b_n grow linearly with the slope $\pi n/\beta$ and the m -dependent intercept. The main effect of mass is non-vanishing $a_n = \tilde{m}(-1)^n$.

value ω_m . Proving this statement or ruling it wrong, is an interesting mathematical question. In the Appendix E.5 we argue that staggering, i.e. the difference between c_e and c_o in (3.1), can not be deduced from the structure of the singularity of $C(t)$ on the complex plane, unlike the mean value $(c_e + c_o)/2$, which is directly related to the pole structure of $C(t)$ at $t = i\beta/2$, i.e. the dimension of the operator ϕ .

For free fields, non-zero particle mass automatically translates into “mass gap” at the level of f^2 . When particles are massive but interact, $f^2(\omega \rightarrow 0)$ will not be zero, although will be exponentially small.⁵ It is an interesting question to understand if this behavior will have any obvious imprint on b_n , and consequently on Krylov complexity.

In the case of persistent staggering exponential growth of $K(t)$ was verified numerically. We leave it as another open question to develop an analytic approximation to evaluate λ_K in terms of β, c_1, c_2 .

4 CFTs on a sphere

In this section we consider a CFT placed on a sphere and calculate Lanczos coefficients and Krylov complexity associated with the Wightman-ordered thermal two-point function. We consider two cases, 4d free massless scalar on \mathbb{S}^3 and holographic theories.

⁵We thank Luca Delacretaz for bringing this point to our attention.

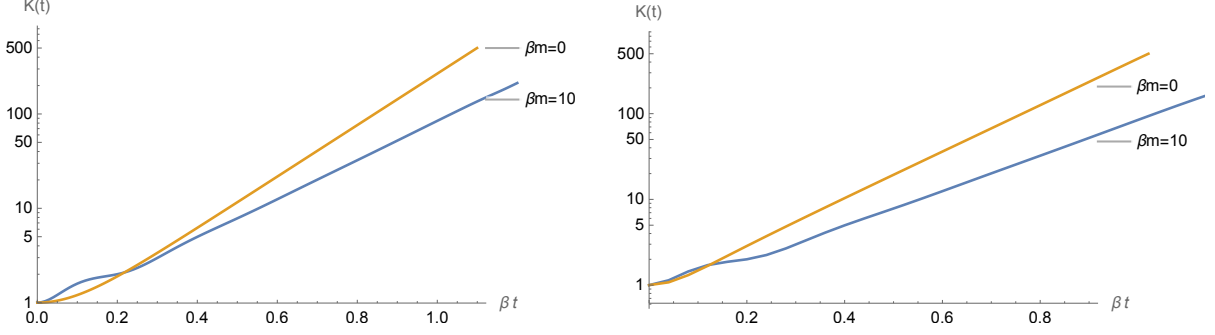


Figure 2. Krylov complexity for the free massive scalar (left) and fermion (right) in $d = 4$ dimensions. For the massless scalar $K = 1 + 2 \sinh^2(\pi t/\beta)$ is known analytically. The main effect of mass is the decrease of Krylov exponent λ_K .

4.1 Free scalar on $\mathbb{S}^3 \times \mathbb{S}^1$

We first consider a 4d free massless scalar compacted on a three-sphere. Because we are considering a finite-temperature correlation function, the 4d compactification manifold is $\mathbb{S}^3 \times \mathbb{S}^1$. Corresponding thermal two-point function is given by, see Appendix C,

$$C(\tau, R) \propto \sum_{n, \ell \in \mathbb{Z}} \frac{(\tau + 1/2 + n)^2 - (R\ell)^2}{((\tau + 1/2 + n)^2 + (R\ell)^2)^2} = \quad (4.1)$$

$$\sum_{\ell \in \mathbb{Z}} \frac{\pi^2}{2} \left(\frac{1}{\cosh^2(\ell\pi R + i\pi\tau)} + \frac{1}{\cosh^2(\ell\pi R - i\pi\tau)} \right) - \frac{2\pi}{R} = \quad (4.2)$$

$$\sum_{n \in \mathbb{Z}} \frac{\pi^2}{R^2} \frac{1}{\sinh^2((n + 1/2 + \tau)\pi/R)}. \quad (4.3)$$

Here R is the radius of \mathbb{S}^3 measured in the units of β , which is the radius of \mathbb{S}^1 . In other words, without loss of generality, we can take $\beta = 1$. Euclidean time τ is defined as $\tau = it/\beta$. As expected, the function is periodic in Euclidean time $\tau \rightarrow \tau + 1$, but it is also periodic in Lorentzian time under $t \rightarrow t + R$, which follows e.g. from (4.3).

For any finite R , Lanczos coefficients split into even and odd branches, which grow linearly with n but with different slopes, see Fig. 3. This can be seen analytically in the limit $R \rightarrow 0$ when $C(\tau)$ is exponentially small (unless $|\tau| = 1/2$) and Lanczos coefficients, at leading order, are given by

$$b_n^2 = \left(\frac{2\pi}{R} \right)^2 \begin{cases} (n+1)^2/4, & n = 1, 3, 5, \dots \\ \frac{4n(n+1)^2}{n+2} e^{-\pi/R}, & n = 2, 4, 6, \dots \end{cases} \quad (4.4)$$

Numerically, this approximation is good already for $R \lesssim 1$.

In the opposite limit of large \mathbb{S}^3 the correlation function approaches that one of flat space, plus a correction $-2\pi/R$, plus the exponentially suppressed terms

$$C \propto \frac{\pi^2}{\cos^2(\pi\tau)} - \frac{2\pi}{R} + \frac{\pi^2}{\cosh^2(\pi R - i\pi\tau)} + \frac{\pi^2}{\cosh^2(\pi R + i\pi\tau)} + \dots \quad (4.5)$$

The exponentially suppressed terms are important for the asymptotic behavior of b_n . Neglecting them, i.e. keeping only first two terms in (4.5) yields the following expression for Lanczos coefficients, which we denote b_n^0 ,

$$(b_n^0)^2 = \pi^2 n(n+1) - (-1)^n \frac{c_n^2}{c_n R + d_n}, \quad n \geq 1, \quad (4.6)$$

$$c_n = \pi(2n+1 - (-1)^n), \quad d_n = 4 \left\lfloor \frac{n+1}{2} \right\rfloor \left(\psi^{(0)}\left(\frac{3}{2}\right) - \psi^{(0)}\left(\left\lfloor \frac{n+1}{2} \right\rfloor + \frac{1}{2}\right) - 2 \right).$$

Here ψ^0 is a polygamma function. This expression has incorrect asymptotic behavior for large n . Taking into account two more terms in (4.5) leads to

$$b_n^2 = (b_n^0)^2 + 8\pi^2 (-1)^n n(n+1)(2n+1) e^{-2\pi R} + O(e^{-\pi R}/R), \quad n \geq 1, \quad (4.7)$$

which still has incorrect the asymptotic. We thus conclude that to reproduce “two slopes” behavior

$$b_n = \begin{cases} \alpha_{\text{odd}}(n + c_1) + o(n), & \text{odd } n, \\ \alpha_{\text{even}}(n + c_2) + o(n), & \text{even } n, \end{cases} \quad n \gg 1. \quad (4.8)$$

would require taking into account an infinite series of ever more exponentially suppressed terms into account. For all finite R , $\alpha_{\text{odd}} > \alpha_{\text{even}}$; the opposite would contradict $C(t \rightarrow \infty) \rightarrow 0$.⁶ The ratio $\alpha_{\text{odd}}/\alpha_{\text{even}}$ grows with R^{-1} , when radius is large two slopes are almost equal to each other and π/β , see section E.4, but for small R they are significantly different, with α_{even} quickly approaching zero. We also show in full generality in the Appendix E.2, that in case of two-slopes behavior (4.8), the inequality $\alpha_{\text{odd}} \geq \pi/\beta \geq \alpha_{\text{even}}$ always holds, see (E.33).⁷

Now we discuss Krylov complexity, which we calculate numerically. We find that $K(t)$ first increases, but then reaches its maximum and starts oscillating periodically, with the same period $T = R$ as $C(t)$, see the right panel of Fig. 3. This behavior is more pronounced for small R , while for a large radius the behavior of $K(t)$ initially follows the flat space counterpart $K(t) = 1 + 2 \sinh^2(\pi t)$, before peaking at some finite value of order $e^{aR/\beta}$, where a is a numerical coefficient of order one.

⁶This follows from the existence of a normalized zero mode of the Liouvillian, provided asymptotically, for odd n , $b_n/b_{n+1} < 1$.

⁷In Appendix, we show for two slopes behavior, that $\alpha_1 \geq \pi/\beta \geq \alpha_2$, where $\alpha_1 = \max(\alpha_{\text{even}}, \alpha_{\text{odd}})$ and $\alpha_2 = \min(\alpha_{\text{even}}, \alpha_{\text{odd}})$. The condition $\alpha_{\text{odd}} \geq \alpha_{\text{even}}$ follows separately from $C(t \rightarrow \infty) \rightarrow 0$, as mentioned above.

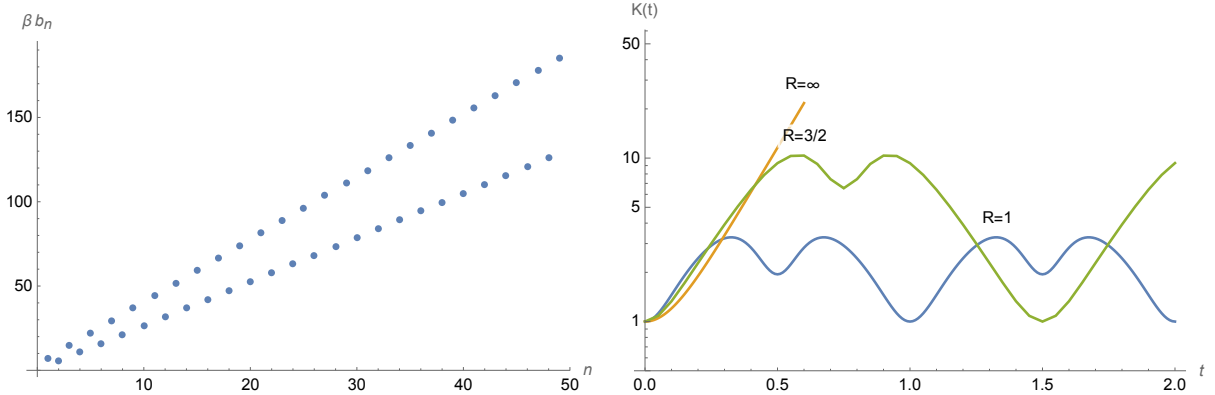


Figure 3. Left: Lanczos coefficients for free massless scalar compactified on \mathbb{S}^3 of radius $R = 1$. Right: Krylov complexity $K(t)$ for radii $R = 1$, flat space $K = 1 + 2 \sinh^2(\pi t/\beta)$, and $R = 3/2$. Because of the periodicity of $C(t)$, it is periodic with the period $T = R$.

The two slopes behavior of b_n is a novel phenomenon, not observed for physical systems previously. This goes beyond the universal operator growth hypothesis of [1], which assumes a smooth asymptote of b_n . Similarly, capped Krylov complexity with the maximal value dependent on R (the ratio of \mathbb{S}^3 and \mathbb{S}^1 radii), but independent of the UV-cutoff is in tension with the proposal that qualitatively $K(t)$ is similar to holographic and computational complexities [27, 29, 30]. In the latter case, for a QFT on compact space, complexity would grow up to exponentially large values, controlled by the volume of \mathbb{S}^3 measured in the units of the UV cutoff. In case of $K(t)$ this growth was presumably supposed to come from the region of b_n which is controlled by UV physics (and where b_n are approximately constant while $K(t)$ grows linearly, see sections 5.2, 5.3 and Figs. 5 and 6). But the example above shows that the operator can be confined at the beginning of “Krylov chain,” in which case the values of b_n for large n do not matter.

Physically, it is tempting to relate the two slopes behavior of b_n and bounded $K(t)$ to the finite volume of the space QFT is placed on, but we will see in the next section this is not true in full generality.

Mathematically, the two slopes behavior of b_n is probably due to periodicity of $C(t)$ in Lorentzian time, or more broadly due to $f^2(\omega)$ being a sum of delta-functions for a not necessary periodic grid of values of ω . We leave a proper investigation of this question for the future, together with the question of quantitatively relating $\alpha_{even}, \alpha_{odd}$ to properties of $C(t)$. Here we only make one step in this direction and use the integral over Dyck paths developed in [3] to relate a particular combination of $\alpha_{even}, \alpha_{odd}$ to the location of the singularity of $C(t)$ in the complex plane, see Appendix E. Another

question, which we also leave for the future, is to analytically relate maximal or time-averaged value of $K(t)$ to values of $\alpha_{even}, \alpha_{odd}$.

4.2 Holographic theories

Next we consider a holographic theory with the two-point function of heavy operators given by the sum over geodesic lengths in thermal AdS space, or black hole background, below and above the Hawking-Page transition correspondingly. In the former case the two-point function is⁸

$$C(t) \propto \sum_n \frac{1}{(\cosh((\tau + 1/2 + n)\beta) - 1)^\Delta} \quad (4.9)$$

where the radius of the boundary sphere is taken to be one. This expression is valid for all Δ , not necessarily large, see e.g. [53]. This expression is valid in all dimensions $d \geq 3$. We notice that, again, besides periodicity in Euclidean time $\tau \rightarrow \tau + 1$, this function is periodic in Lorentzian time $t \rightarrow t + 2\pi$. This is presumably the reason why b_n behave qualitatively the same as in the previous subsection – they split into two branches for even and odd n , with both exhibiting asymptotic linear growth (4.8). The behavior of Krylov complexity also follows the pattern of free scalar on \mathbb{S}^3 , it first grows but then oscillates periodically, see Fig. 4. We thus conclude that in holographic theories Krylov complexity can be UV-independent, thus making it qualitatively different from the holographic complexity [8–14].

The discussion above applies to temperatures small enough, below the Hawking-Page transition. As the temperature increases the dual geometry is given by the BTZ background, assuming we focus specifically on the case of 2d theories. The two-point function in this background is given by [54, 55]

$$C(t) \propto \sum_n \frac{1}{(\cos(2\pi\tau) + \cosh(4\pi^2 n/\beta))^\Delta}. \quad (4.10)$$

This function is, of course, periodic under $\tau \rightarrow \tau + 1$, but there is no periodicity in Lorentzian time. As a result Lanczos coefficients have the “vanilla” behavior, growing linearly with the asymptote (2.9). In fact, the leading contribution comes from the $n = 0$ term in (4.10), which is the same as the flat-space expression, with other terms for $\beta < 2\pi$ giving very small corrections. We find numerically b_n^2 to be very close to the flat space result, $\pi^2(n+1)(n+2\Delta)/\beta^2$ [4]. Accordingly, Krylov complexity grows exponentially with $\lambda_K = 2\pi/\beta$.

⁸We thank Matthew Dodelson for the collaboration that laid the foundation for results of this section.

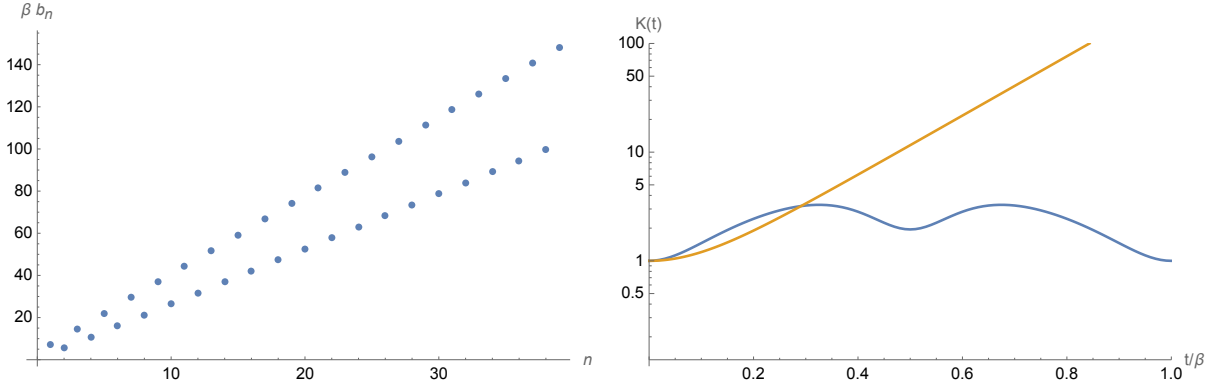


Figure 4. Left: Lanczos coefficients for thermal AdS background (4.9) with $\beta = 2\pi$ and $\Delta = 1$. Right: Krylov complexity for these parameters (blue) superimposed with the flat space 2d CFT behavior $K = 1 + 2 \sinh^2(\pi t/\beta)$ (orange). Because of periodicity of $C(t)$, blue curve is also periodic with $K(t) = K(t + 2\pi)$.

The calculation in the BTZ background shows that two slopes behavior and capped $K(t)$ are not universal features of QFT on compact spaces, and the unbounded exponential growth of $K(t)$ is possible in the holographic settings. This prompts the question of how the inequality (1.1) fares in different holographic scenarios. We see that above the Hawking-Page transition Krylov exponent λ_K is well defined and equal to $2\pi/\beta$. This means the second inequality in (1.1) is saturated and reduces to the Maldacena-Shenker-Stanford bound, which is also saturated by holographic theories. Below the transition, Krylov complexity is bounded, hence λ_K is not well-defined, or we can formally take it equal to zero. Exactly in the same scenario the OTOC correlator exhibits periodic recurrences [56]. As we mentioned in the introduction, in this case we assign $\lambda_{\text{OTOC}} = 0$. In other words, (1.1) remains valid in both cases.

5 Temperature and UV-cutoff dependence of Lanczos coefficients

We have seen in the previous sections that giving particles mass or placing a CFT on a compact background both have an explicit imprint on Lanczos coefficients and Krylov complexity. One feature, which nevertheless seems to be lost in the QFT case is the sensitivity of b_n to chaos. Indeed, in all cases above b_n exhibit linear growth (albeit sometimes by splitting into two branches), even though many considered theories are not chaotic. This mirrors the behavior we previously observed for CFTs in flat space [4] and complements recent observation that non-chaotic systems with saddle-dominated scrambling also exhibit linear growth of b_n [5].

This could be our final conclusion – that asymptotic of Lanczos coefficients is not a proper probe of chaos, but apparent success of this approach in case of discrete systems with finite local Hilbert space, in particular spin chains, hints this conclusion could be premature. As we mentioned above, for 1D lattice systems the slowest possible decay of $f^2(\omega)$ is not exponential but super-exponential $f^2(\omega) \sim \omega^{-\omega}$ [3]. Yet for integrable spin chains $f^2(\omega)$ decays faster, as a Gaussian (which correspond to asymptotic growth $b_n \propto n^{1/2}$) or even becomes zero for ω exceeding certain size-independent threshold. This is the case in all known examples, including preliminary numerical evidence for the XXZ model [57]. On the contrary for the non-integrable 1d Ising model in transverse field it was recently proved in [58] that f^2 will decay with the slowest possible asymptotic, $f^2(\omega) \propto \omega^{-\omega}$. These results constitute non-trivial evidence for the “asymptotic of b_n as a probe of chaos” stronger version of the universal operator growth hypothesis.⁹ We should mention, there is an additional evidence for this hypothesis for $D > 1$ lattice models: an analytic proof of $f^2 \propto e^{-\omega/\omega_0}$ asymptotic for a non-integrable 2D lattice model [59], and for the limit of SYK model [1].

Apparent success with the spin chains and other discrete models and failure in field theoretic models suggest the issue could be related to the continuous nature of the latter. We elaborate on this in the next section.

5.1 Asymptotic of $f^2(\omega)$ and locality

While for spin chains high frequency asymptotic of f^2 apparently contains some dynamical information, for continuous systems it is completely universal. Let’s consider the power spectrum, the Fourier transform of two-point correlation function in field theory. The power spectrum $f^2(\omega)$ has a simple interpretation as the sum of transition amplitudes between the one-particle states with energies E_i and energies $E_f = E_i + \omega$. Its high-frequency asymptotic can be deduced from the following consideration. Let us consider a free quantum-mechanical particle propagating in 1D. Assuming the particle is fully localized, the Heisenberg uncertainty principle implies the transition amplitude to a state with arbitrarily high energy is not suppressed (the Fourier transform of the delta-function is a constant). After restoring β -dependent factors this means $f^2(\omega)$ will be proportional to $e^{-\beta\omega/2}$. Here locality of the initial state was crucial for the transition amplitude to states with large final energy to be unsuppressed. Going back to the two-point function $C(t)$, this translates into locality of the operator A . To see this in more detail, let us consider a simple example, free quantum-mechanical particle with

⁹The original hypothesis claimed that a generic system would feature maximal possible growth of b_n .

the Hamiltonian $H = \frac{p^2}{2m}$, and an operator in the Heisenberg picture

$$A = e^{-x^2/a}. \quad (5.1)$$

We would like to evaluate (2.6) and find

$$f^2(\omega) = K_0(\sqrt{\beta(\beta + 4am)}\omega/2). \quad (5.2)$$

It's clear that when a is large, which corresponds to a de-localized wave-packet, the decay of f^2 is *faster* than the kinematically fixed value $f^2 \propto e^{-\beta\omega/2}$ associated with the point-like operator $a \rightarrow 0$.

Provided the logic above is correct we may expect that in the case of translationally-invariant lattice models similar behavior will emerge in the continuous (long wave) approximation, emerging in the low energy (low temperature) limit. We test this below in case of bosonic and fermionic lattice models. For the fixed value of coupling constants, effective wavelength is specified by inverse temperature β . Thus we expect that for large β an approximate continuous description will emerge, leading to universal high frequency tail of f and universality of b_n behavior. On the contrary, for small β we expect to recover the diversity of b_n behaviors previously observed in the literature, and in particular connection between the asymptotic of b_n and chaos.

5.2 Integrable XY model at finite temperature

The integrable periodic XY spin chain

$$H = \sum_{i=1}^N (1 + \gamma) S_i^x S_{i+1}^x + (1 - \gamma) S_i^y S_{i+1}^y - h S_i^z \quad (5.3)$$

is solvable through the Jordan-Wigner transform and the two-point function at finite temperature

$$C(t) = \langle S^z(t) S^z(0) \rangle_\beta^W = \text{Tr}(e^{-\beta H/2} S^z(t) e^{-\beta H/2} S^z) \quad (5.4)$$

is known explicitly, see Appendix D. We are interested in the thermodynamic limit of infinite N and start with the case of isotropic XY model with $\gamma = h = 0$, in which case

$$C(\tau) = \frac{1}{4\pi^2} \left(\int_{-1}^1 \frac{dc}{\sqrt{1-c^2}} \frac{\cosh(c\tau)}{\cosh(c\beta/2)} \right)^2. \quad (5.5)$$

Calculating b_n numerically, for different values of β reveals the following behavior. Initially Lanczos coefficients grow linearly as $b_n \approx \pi n/\beta$, and then saturate at some universal value $b_n \approx 1$, see Fig. 5. Clearly, initial region of linear growth increases

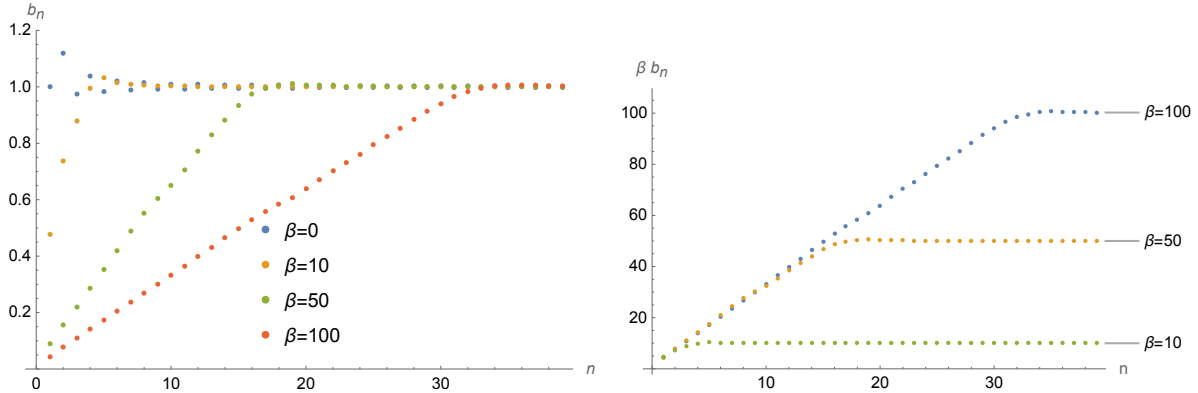


Figure 5. Both panels: Lanczos coefficients for the isotropic XY model (5.5).

for larger β . This has the following interpretation, at small temperatures the isotropic XY model becomes the free fermion CFT, hence Lanczos coefficients exhibit universal vanilla CFT behavior (2.9). For large n , when b_n (which have dimension of energy) become of the order of UV-cutoff (which is of order one in our case), the universal QFT behavior is substituted by the true asymptotic behavior reflecting the dynamics of the lattice model. Since the isotropic XY model is free, Lanczos coefficients saturate at a fixed value, in full agreement with the previous observations that the asymptotic of b_n is a probe of chaos (or lack thereof).

The main takeaway here is that to probe chaos of the underlying lattice model, one should consider true asymptotic behavior of b_n which is controlled by UV-cutoff physics. In the QFT models with an infinite cutoff, such as conformal field theories, the true asymptote is not accessible, giving way to essentially universal vanilla behavior (of one or two linearly growing branches of b_n).

5.3 Free bosons on the lattice

Next we consider free oscillators on the 1D lattice with periodic boundary conditions,¹⁰

$$H = \frac{1}{4} \sum_{i=1}^N \pi_i^2 + (\phi_{i+1} - \phi_i)^2 + 4\mu^2 \phi_i^2, \quad (5.6)$$

which becomes 1D free massive scalar theory in the continuous limit. We can think of this model as the 1+1 free scalar QFT with a UV cutoff. In the thermodynamic limit $N \rightarrow \infty$, when the mass μ and temperature β^{-1} are chosen to be much smaller than the cutoff, $\beta \gg 1 \gg \mu$, we expect the CFT in flat space behavior with $f^2 \propto e^{-\beta\omega/2}$ and

¹⁰Scalar field with UV-cutoff was also considered in [49].

linearly growing Lanczos coefficients $b_n \sim \pi n/\beta$. At high energies we are dealing with the discrete integrable model of non-interacting particles with the energies belonging to a finite width zone. Accordingly $f^2(\omega)$ vanishes for ω exceeding certain value ω^* . Thus, similarly to the isotropic XY model considered above, Lanczos coefficients are expected to approach a constant, signaling lack of chaos.

If N is finite, in the long-wave limit the system is described by free massive QFT placed on \mathbb{S}^1 . In other words, the model (5.6) includes all three deformations we discuss in the paper: the mass, compact spatial manifold and the UV-cutoff. Accordingly, depending on the interplay between β, μ and N , at the level of b_n we expect to see the combinations of some or all three features: persistent staggering, two-slopes behavior (since the theory is free, and the spectrum of excitations is equally-spaced), and field theory behavior below and saturation of b_n near the UV-cutoff. An explicit calculation of (2.6) yields

$$C(\tau) \propto \frac{1}{N} \sum_{k=1}^N \frac{1}{\epsilon_k} \frac{\cosh(\epsilon_k \tau)}{\sinh(\epsilon_k \beta/2)}, \quad \epsilon_k = \sqrt{\sin^2(k) + \mu^2}, \quad k = \pi k/N. \quad (5.7)$$

and the behavior of Lanczos coefficients for different β, N and $\mu \ll 1$ is shown in Figure 6.

As expected, for essentially infinite N and large β initially b_n grow linearly, as $b_n \approx \pi n/\beta$, but once the value of b_n becomes the order of the cutoff (which is of order one in our case), they saturate to a constant. The punchline here is clear: for small temperatures the prolonged universal linear growth of b_n , dictated by the locality and Heisenberg uncertainty principle, will eventually give way to true asymptotic behavior governed by the discrete model emerging at the UV-cutoff scale. When N is finite we observe the two slopes behavior, on top of the persistent staggering due to mass, and the transition toward true asymptote due to UV-cutoff.¹¹

6 Discussion

In the paper we calculated Lanczos coefficients b_n and Krylov complexity $K(t)$ of local operators in several models of quantum field theory, free massive scalars and fermions, massless scalars compactified on a sphere, and a few holographic examples. Our calculations revealed that all three deformations of CFTs in flat space: giving particle mass, placing theory on a compact space, and introducing finite UV-cutoff has a clear imprint on b_n and $K(t)$. Namely, mass leads to persistent staggering of b_n (3.1) and decreases

¹¹In this case $C(t)$ is not periodic in Lorentzian time, but for any finite N , $f^2(\omega)$ has finite support, which is perhaps behind the two slopes behavior, clearly visible in Fig. 6.

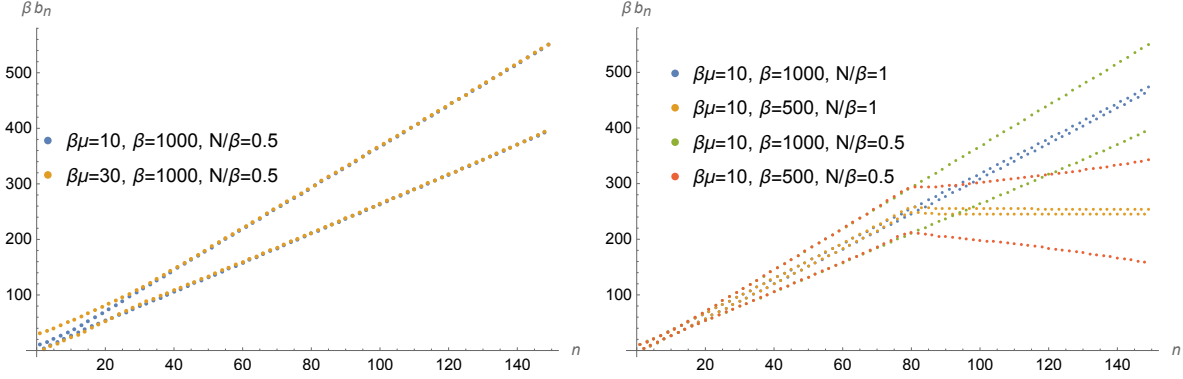


Figure 6. Lanczos coefficients for free bosons on the lattice (5.6) for different values of β, μ, N parameters. For large β initial behavior of b_n like the one in field theory – coefficients grow linearly, either demonstrating persistent staggering and/or two-slopes behavior, see left panel. When b_n approach UV-cutoff value the QFT behavior changes into one governed by the UV physics, see right panel.

the Krylov exponent λ_K , while $K(t)$ still grows exponentially. Compact space, at least in certain cases, leads to two sloped behavior (4.8) and a capped Krylov complexity. Finite cutoff introduces a new asymptotic regime, where b_n behavior is controlled by the lattice model at the UV scale.

These examples help us formulate several takeaway messages, clarifying the universal operator growth hypothesis of [1] and the role of Krylov complexity. First, asymptotic behavior of b_n in physical systems goes beyond universality previously discussed in the literature, namely b_n can split into two branches for even and odd n , each with its own asymptotic behavior. In particular this means that asymptotic behavior of b_n is not mathematically equivalent or fully controlled by the high frequency asymptote of $f^2(\omega)$. Second, we clarified the role of temperature for b_n in lattice models. Third, in field theory with an infinite UV-cutoff Lanczos coefficients do not probe chaotic behavior. But when a finite cutoff Λ_{UV} is introduced, by embedding the QFT into a lattice model, a true asymptotic regime of $b_n \gtrsim \Lambda_{UV}$ emerges, which is conjecturally probing chaos in the underlying lattice model, modulo issues raised in [5]. Here it is worth noting that a chaotic QFT can not emerge as a long wave limit from an integrable lattice model. Thus, with the help of a finite UV-cutoff, the universal operator growth hypothesis can be extended to quantum field theories.

Another takeaway message is the generalization of the Maldacena-Shenker-Stanford bound (1.1), which we tested in several non-trivial settings.

Finally, the examples of theories demonstrating two slopes behavior of b_n and a capped $K(t)$ clearly show, Krylov complexity can have qualitatively different behavior

than the holographic and computational, e.g. Nielsen, complexity [8–14, 31, 60].

Our work raises numerous questions, including a number of mathematical questions about the relation between b_n and $C(t)$. Among them are the features of $C(t)$ which lead to asymptotic persistent staggering (3.1) or two slopes (4.8) behavior and how to deduce $\alpha_o, \alpha_e, c_o, c_e$ from $C(t)$. Here we presume a simple generalization of (2.9) is possible, though in section 4.1 we saw the example when the asymptotic of b_n was dependent on the exponentially suppressed contributions to $C(t)$. There are many other questions, how to quantitatively relate λ_K to c_o, c_e in case of persistent staggering, and how to relate maximal or time-averaged $K(t)$ to α_o, α_e in case of two slopes behavior. There are also questions about the physics of Krylov complexity. Can we prove generalized Maldacena-Shenker-Stanford bound (1.1) in full generality? Is there any holographic counterpart of $K(t)$? What is the behavior of b_n and $K(t)$ in interacting QFTs? We leave these and other questions for the future.

Acknowledgments

We thank Dmitri Trunin for collaboration at the early stages of this project, and Luca Delacretaz, Matthew Dodelson, Oleg Lychkovskiy, Julian Sonner, Subir Sachdev, Adrian Sanchez-Garrido, and Erez Urbach for discussions. AA acknowledges support from a Kavli ENSI fellowship and the NSF under grant number DMR-1918065. AD is supported by the National Science Foundation under Grants PHY-2013812 and 2310426.

A Massive free theories

A.1 Massive scalar

We start with a free massive scalar in \mathbb{R}^d and calculate thermal two-point function

$$\langle \phi(\tau)\phi(-1/2) \rangle_\beta = \sum_{n=-\infty}^{\infty} \frac{(-1)^n}{\beta} \int \frac{d^{d-1}k}{(2\pi)^{d-1}} \frac{e^{i2\pi n\tau}}{\left(\frac{2\pi n}{\beta}\right)^2 + k^2 + m^2}. \quad (\text{A.1})$$

Here $\tau = it/\beta$ is the Euclidean time. One operator is placed at $\tau = -1/2$, thus this is a Wightman-ordered correlator .

$$\langle \phi(\tau)\phi(-1/2) \rangle_\beta \propto \text{Tr}(e^{-\beta H/2}\phi(t, x)e^{-\beta H/2}\phi(0, x)).$$

To evaluate (A.1) we substitute the sum over n by a contour integral going over the singularities of $\sinh\left(\frac{\tilde{k}_0}{2}\right)$,

$$\langle \phi(\tau)\phi(-1/2) \rangle_\beta = \frac{\beta^{2-d}}{4\pi i} \int_{\mathcal{C}} d\tilde{k}_0 \int \frac{d^{d-1}\tilde{k}}{(2\pi)^{d-1}} \frac{e^{\tilde{k}_0\tau}}{\sinh\left(\frac{\tilde{k}_0}{2}\right)(\tilde{m}^2 + \tilde{k}^2 - \tilde{k}_0^2)}. \quad (\text{A.2})$$

The contour can be deformed and closed through the infinite semicircle at $\text{Re}\tilde{k}_0 \rightarrow \infty$, yielding

$$C(t) = \text{Tr}(e^{-\beta H/2}\phi(t, x)e^{-\beta H/2}\phi(0, x)) \propto \frac{\beta^{2-d}}{(4\pi)^{\frac{d-1}{2}}\Gamma(\frac{d-1}{2})} \int_{\tilde{m}}^{\infty} (y^2 - \tilde{m}^2)^{\frac{d-3}{2}} \frac{\cosh(y\tau)}{\sinh(y/2)} dy.$$

A.2 Massive fermion

Similarly for the massive fermion

$$\langle \psi_{\alpha}^{\dagger}(\tau)\psi_{\sigma}(-1/2) \rangle_{\beta} = \frac{1}{\beta} \int \frac{d^{d-1}k}{(2\pi)^{d-1}} \sum_{n=-\infty}^{\infty} \frac{(-1)^n (\pi(2n+1)\delta_{\alpha\sigma} + i\tilde{m}\gamma_{\alpha\sigma}^0) e^{i\pi(2n+1)\tau}}{\left(\frac{(2n+1)\pi}{\beta}\right)^2 + k^2 + m^2} \quad (\text{A.3})$$

We work in Dirac representation such that $\gamma_{\alpha\sigma}^0 = \pm\delta_{\alpha\sigma}$ and use the same trick with the contour integral

$$\langle \psi_{\alpha}^{\dagger}(\tau)\psi_{\sigma}(-1/2) \rangle_{\beta} = \frac{\beta^{1-d}}{4\pi i} \int_{\mathcal{C}} d\tilde{k}_0 \int \frac{d^{d-1}\tilde{k}}{(2\pi)^{d-1}} \frac{(\tilde{k}_0 \pm \tilde{m}) e^{\tilde{k}_0\tau}}{\cosh\left(\frac{\tilde{k}_0}{2}\right) (\tilde{k}^2 + \tilde{m}^2 - \tilde{k}_0^2)}. \quad (\text{A.4})$$

After deforming the integration contour we arrive at

$$\text{Tr}(e^{-\beta H/2}\psi^{\dagger}(t, x)e^{-\beta H/2}\psi(0, x)) \propto \frac{\beta^{1-d}}{(4\pi)^{\frac{d-1}{2}}\Gamma(\frac{d-1}{2})} \int_{|\tilde{m}|}^{\infty} dy (y^2 - \tilde{m}^2)^{\frac{d-3}{2}} \frac{y \cosh(y\tau) \pm \tilde{m} \sinh(y\tau)}{\cosh\left(\frac{y}{2}\right)}.$$

B Lanczos coefficients for general $C(t)$

In the most general case, when $C(t)$ is not a real-valued even function, besides coefficients b_n , Lanczos coefficients also include a_n . Their definition in terms of Krylov basis can be found in e.g. [17], and the explicit expression in terms of $C(t)$ is as follows. For the analytically continued $C(\tau)$, $\tau = it$, we first define an $n \times n$ Hankel matrix of derivatives $\mathcal{M}_{ij}^{(n)} = C^{(i+j)}(\tau)$ and variables $\tau_n = \det \mathcal{M}^{(n)}$, $\tau_0 \equiv 1$. Then

$$b_n = \left. \frac{\tau_{n-1}\tau_{n+1}}{\tau_n^2} \right|_{\tau=0}, \quad (\text{B.1})$$

$$a_n = \left. \frac{d}{d\tau}(\tau_n - \tau_{n-1}) \right|_{\tau=0}. \quad (\text{B.2})$$

C Free scalar on $\mathbb{S}^{d-1} \times \mathbb{S}^1$

Let us consider a compact space \mathbb{S}^{d-1} of radius R . The thermal correlation function of the scalar field living on $\mathbb{R} \times \mathbb{S}^{d-1}$ can be expressed in terms of the heat kernel $K_{\mathcal{M}}(t, x, y) = \langle x | \exp(-t\hat{D}) | y \rangle$, see e.g., [61]

$$\langle \phi(x)\phi(y) \rangle_{\beta} = \int_0^{\infty} dt K(t, x, y) e^{-tm_{\text{eff}}^2}, \quad (\text{C.1})$$

where $\mathcal{M} = \mathbb{S}^1 \times \mathbb{S}^{d-1}$ (\mathbb{S}^1 represents a thermal circle parametrized by τ), and \hat{D} is the second order differential operator of the Laplace-Beltrami type,

$$\hat{D} = -\frac{d}{d\tau^2} - \Delta_{\mathbb{S}^{d-1}} , \quad (\text{C.2})$$

where $\Delta_{\mathbb{S}^{d-1}}$ is the scalar Laplacian on a sphere. Finally m denotes the 'effective' mass of the field under study

$$m_{\text{eff}}^2 = m^2 + \xi \mathcal{R} \quad (\text{C.3})$$

where $\xi = \frac{d-2}{4(d-1)}$ is the conformal coupling and $\mathcal{R} = \mathcal{R}(\mathbb{S}^{d-1}) = (d-1)(d-2)/R^2$ is the Ricci scalar of the background geometry.

The wave operators are separable on the product manifold $\mathbb{S}^1 \times \mathbb{S}^{d-1}$ and hence the heat kernel can be expressed as the product of the two individual heat kernels on \mathbb{S}^1 and \mathbb{S}^{d-1} , i.e.,

$$K_{\mathcal{M}} = K_{\mathbb{S}^1} K_{\mathbb{S}^{d-1}} \quad (\text{C.4})$$

$K_{\mathbb{S}^1}$ can be readily evaluated using the method of images. It is given by an infinite sum of the scalar heat kernels on \mathbb{R} , which are shifted by integer multiples of β with respect to each other to maintain periodic boundary conditions for the scalar field on a circle, namely

$$K_{\mathbb{S}^1}(t, \tau) = \frac{1}{\sqrt{4\pi t}} \sum_{n=-\infty}^{\infty} e^{-\frac{(\tau+n\beta)^2}{4t}} \quad (\text{C.5})$$

In fact, the heat kernel $K_{\mathbb{S}^{d-1}}$ is also known in full generality [62], e.g.,

$$K_{\mathbb{S}^3}(t, x, x) = \frac{e^{t/R^2}}{(4\pi t)^{3/2}} \sum_{n=-\infty}^{\infty} e^{-\frac{\pi^2 R^2 n^2}{t}} \left(1 - 2\frac{\pi^2 R^2 n^2}{t}\right). \quad (\text{C.6})$$

In $d = 4$, we thus get

$$C_{\phi}(\tau) = \sum_{n,\ell=-\infty}^{\infty} \int_0^{\infty} \frac{dt e^{-tm^2}}{(4\pi t)^2} e^{-\frac{(\tau+n\beta)^2 + (2\pi R\ell)^2}{4t}} \left(1 - 2\frac{\pi^2 R^2 \ell^2}{t}\right), \quad (\text{C.7})$$

Integrating over t , yields

$$C_{\phi}(\tau) = m \sum_{n,\ell=-\infty}^{\infty} \frac{A K_1(Am) - 4B^2 m K_2(Am)}{4\pi^2 A^2} .$$

$$A^2 = (\tau + n\beta)^2 + (2\pi R\ell)^2, \quad B = \pi R\ell . \quad (\text{C.8})$$

For $\beta m, Rm \gg 1$ the sum is dominated by a few terms in the vicinity of $n = \ell = 0$. $C_\phi(\tau)$ simplifies in the case of conformally coupled scalar ($m = 0$)

$$C_\phi(\tau) = \frac{1}{4\pi^2} \sum_{n,\ell=-\infty}^{\infty} \frac{(\tau + n\beta)^2 - (2\pi R\ell)^2}{((\tau + n\beta)^2 + (2\pi R\ell)^2)^2}. \quad (\text{C.9})$$

Upon redefinition $\tau \rightarrow \beta\tau$ and $R \rightarrow \beta R$ we arrive at (4.1).

D Thermal 2pt function in XY model

Consider the Hamiltonian of integrable XY model with periodic boundary conditions, $j = 0$ is the same as $j = N$,

$$H = \sum_{j=1}^N [(1 + \gamma)S_j^x S_{j+1}^x + (1 - \gamma)S_j^y S_{j+1}^y] - h \sum_{j=1}^N S_j^z. \quad (\text{D.1})$$

This chain is diagonalizable by the Jordan-Wigner transform [63], with the quasiparticle energies given by $\epsilon_k = \sqrt{(\cos k - h)^2 + \gamma^2 \sin^2 k}$. Here k varies between 0 to 2π . The autocorrelation function at inverse temperature β is defined as

$$C_\beta^z(t) \equiv \langle S_0^z S_0^z(t) \rangle_\beta = \text{Tr}(e^{-\beta H} S_0^z S_0^z(t)) / \text{Tr}(e^{-\beta H}). \quad (\text{D.2})$$

Before giving the expression for $C_\beta^z(t)$ we first thermal expectation value

$$m_z(h) = \langle S_0^z \rangle_\beta = -\frac{1}{2\pi} \int_0^\pi dk \cos \left\{ \tan^{-1} \left(\frac{\gamma \sin k}{\cos k - h} \right) \right\} \tanh \frac{\beta \epsilon_k}{2}, \quad (\text{D.3})$$

and one can show that $\lim_{h \rightarrow 0} m^z(h) = 0$. Finally, the autocorrelation function is given by

$$C_\beta^z(t) = m_z^2(h) + \left[\frac{1}{2\pi} \int_0^\pi dk \left\{ \cos(\epsilon_k t) + i \sin(\epsilon_k t) \tanh \frac{\beta \epsilon_k}{2} \right\} \right]^2 - \left[\frac{1}{2\pi} \int_0^\pi dk \cos(2\lambda_k) \left\{ i \sin(\epsilon_k t) + \cos(\epsilon_k t) \tanh \frac{\beta \epsilon_k}{2} \right\} \right]^2, \quad (\text{D.4})$$

where $\lambda_k = \frac{1}{2} \tan^{-1} \frac{\gamma \sin k}{\cos k - h}$.

This expression becomes particularly simple, when we set $\gamma = 0$, $h = 0$ which corresponds to isotropic XY model $H = \sum_{j=1}^N [S_j^x S_{j+1}^x + S_j^y S_{j+1}^y]$,

$$C_\beta(t) = \frac{1}{4\pi^2} \left(\int_{-1}^1 \frac{dc}{\sqrt{1-c^2}} \left[\cos(tc) - i \sin(tc) \tanh \frac{\beta c}{2} \right] \right)^2, \quad (\text{D.5})$$

which becomes even simpler upon the shift $t \rightarrow t - i\beta/2$ that gives the Whightman-ordered correlator, cf. with (5.5),

$$C_\beta^W(t) = \frac{1}{4\pi^2} \left[\int_{-1}^1 \frac{dc}{\sqrt{1-c^2}} \frac{\cos(tc)}{\cosh \beta c/2} \right]^2. \quad (\text{D.6})$$

E Dyck paths integral for two slopes scenario

E.1 Integral over Dyck paths formalism for two branches

Here we will generalize the derivation of the asymptotic behavior of moments

$$\mu_{2n} = \int d\omega f^2(\omega) \omega^{2n} \quad (\text{E.1})$$

from [3] to the case when b_n form two continuous branches for large n , $b_{2n} = b_{\text{even}}(2n)$ and $b_{2n+1} = b_{\text{odd}}(2n)$. We also introduce

$$\epsilon(n) = b_{\text{even}}(n)/b_{\text{odd}}(n), \quad (\text{E.2})$$

$$b(n) = \sqrt{b_{\text{even}}(n)b_{\text{odd}}(n)}, \quad (\text{E.3})$$

and assume they are smooth functions of their argument.

We start with the Dyck path sum representation of moments [1]

$$\mu_{2n} = \sum_{\{h_k\} \in D_n} \prod_{k=0}^{2n-1} b_{(h_k+h_{k+1})/2}, \quad (\text{E.4})$$

where D_n is the set of all Dyck paths.

We approximate each Dyck path with $h_i = 1/2 + 2nf(i/2n)$, where $f(t)$ is a continuous function defined on $0 < t < 1$ and satisfying $|f'(t)| < 1$. Let us consider N consecutive steps in a Dyck path, where $h_{k+1} - h_k = 1$ for n distinct values of k so that $f' = \frac{2n-N}{2}$. We additionally require that the index of b is even d times more than it is odd. We split the interval in pairs and we will denote the steps were value of h increased (decreased) as "+" or "-" correspondingly.

For pairs "++" or "--" one factor of b has an odd index and another has an even one. For pairs "+-" and "-+" both factors will have the same parity that depends on the current value of h_i . If we denote the number of "++" pairs as m and the number of opposite sign pairs that lead to two even factors as l we obtain $d = 4l - 2n + 4m$. Assuming our interval is small, its weight in (E.4) is given by

$$b_{\text{odd}}^{N/2-2l+n-2m} b_{\text{even}}^{N/2+2l-n+2m} = \sqrt{b_{\text{odd}} b_{\text{even}}}^N (b_{\text{even}}/b_{\text{odd}})^{2l-n+2m}. \quad (\text{E.5})$$

The parameters satisfy $0 < n < N$, $n - N/2 < m < n/2$ and $0 < l < n - 2m$. The number of paths for fixed n , m and l is given by $C_{N/2}^m C_{N/2-m}^{n-2m} C_{n-2m}^l$. This product can be approximated with the help of the Stirling's formula

$$\log C_{N/2}^m C_{N/2-m}^{n-2m} C_{n-2m}^l \approx \frac{N}{2} \left[S(\alpha) + (1 - \alpha) S\left(\frac{f' + 1 - 2\alpha}{1 - \alpha}\right) + (f' + 1 - 2\alpha) S\left(\frac{\beta}{f' + 1 - 2\alpha}\right) \right], \quad (\text{E.6})$$

where $n = N \frac{f'+1}{2}$, $\alpha = \frac{m}{N/2}$, $\beta = \frac{l}{N/2}$ and

$$S(\alpha) = -\alpha \log \alpha - (1 - \alpha) \log(1 - \alpha). \quad (\text{E.7})$$

We can evaluate the sum over l and m

$$\sqrt{b_{\text{odd}} b_{\text{even}}}^{-N} \sum_{m,l} C_{N/2}^m C_{N/2-m}^{n-2m} C_{n-2m}^l \epsilon^{2l-n+2m}, \quad (\text{E.8})$$

where $\epsilon = b_{\text{even}}/b_{\text{odd}}$ via the saddle point approximation. This is function (E.2), now understood as a smooth function of f , $\epsilon(2nf)$. The function to be minimized is

$$W(\alpha, \beta, f', \epsilon) = S(\alpha) + (1 - \alpha) S\left(\frac{f' + 1 - 2\alpha}{1 - \alpha}\right) + (f' + 1 - 2\alpha) S\left(\frac{\beta}{f' + 1 - 2\alpha}\right) + (2\alpha + 2\beta - f' - 1) \log \epsilon.$$

The saddle point equations are

$$\epsilon^2(1 - 2\alpha - \beta + f')^2 = \alpha(\alpha - f'), \quad (\text{E.9})$$

$$\epsilon^2(1 - 2\alpha - \beta + f') = \beta. \quad (\text{E.10})$$

It is solved by

$$\alpha^* = \frac{f'(1 - \epsilon^2)^2 - 4\epsilon^2 + (1 + \epsilon^2)\sqrt{4\epsilon^2 + (\epsilon^2 - 1)^2 f'^2}}{2(\epsilon^2 - 1)^2}, \quad (\text{E.11})$$

$$\beta^* = \frac{\epsilon^2}{(\epsilon^2 - 1)^2} (1 + \epsilon^2 - \sqrt{4\epsilon^2 + (\epsilon^2 - 1)^2 f'^2}). \quad (\text{E.12})$$

Plugging this back in the expression for W , we obtain

$$W_{\text{eff}}(f', \epsilon) = -\frac{f'}{2} \log \frac{\epsilon^4 f'^2 + f'(f' + \sqrt{4\epsilon^2 + (\epsilon^2 - 1)^2 f'^2}) + \epsilon^2(2 + f' \sqrt{4\epsilon^2 + (\epsilon^2 - 1)^2 f'^2})}{2\epsilon^2(1 - f')^2} + 2 \log(1 + \epsilon) + \log \frac{(\epsilon^2 - 1)^2}{\epsilon + \epsilon^3 - \epsilon \sqrt{4\epsilon^2 + (\epsilon^2 - 1)^2 f'^2}}. \quad (\text{E.13})$$

As expected, W_{eff} is invariant under $\epsilon \rightarrow 1/\epsilon$, which emphasizes that both branches are on the same footing. In what follows we take $0 \leq \epsilon \leq 1$, by assuming that α_{odd} is the slope of the faster growing branch and α_{even} is the slope of the slower growing branch, with no reference to whether corresponding n is even or odd.

Finally, this gives us a path integral representation of moments (E.1) in terms of smooth functions (E.2,E.3)

$$\mu_{2n} = \int \mathcal{D}f(t) e^{n \int_0^1 dt (W_{\text{eff}}(f', \epsilon(2nf)) + 2 \log b(2nf))}. \quad (\text{E.14})$$

We can verify that this path integral reduces to the path integral for a single branch developed in [3] when we set $\epsilon = 1$ ($b_{\text{even}} = b_{\text{odd}}$). While the second term is singular as $\epsilon \rightarrow 0$ it is finite if we carefully take the limit

$$\lim_{\epsilon \rightarrow 1} W_{\text{eff}}(f', \epsilon) = 2S \left(\frac{f' + 1}{2} \right). \quad (\text{E.15})$$

Alternatively, the saddle point configuration simplifies to

$$\alpha^* = \frac{(1 + f')^2}{4}, \quad \beta^* = \frac{(1 - f')^2}{4}. \quad (\text{E.16})$$

and again we obtain $W(\alpha^*, \beta^*, f', 1) = 2S \left(\frac{f'+1}{2} \right)$. This agrees with the expected result, since W is multiplied by n (it used to be $2n$ in the single branch case).

E.2 Evaluation of the path integral for two slopes

Here we assume that $\epsilon = \text{const}$ and $\sqrt{b_{\text{odd}}(n)b_{\text{even}}(n)} = \alpha n$. The action in this case reads

$$I = \int_0^1 dt (W_{\text{eff}}(f', \epsilon) + 2 \log f), \quad (\text{E.17})$$

where we have neglected the constant term $2 \log(2\alpha n)$ in the integral since it does not affect the shape of the saddle point. Varying I with respect to $f(t)$, we obtain the EOMs

$$-\frac{2}{f(t)} = \frac{f''}{1 - (f')^2} \frac{(1 + \epsilon^2 + \sqrt{4\epsilon^2 + (-1 + \epsilon^2)^2 (f')^2})}{\sqrt{4\epsilon^2 + (-1 + \epsilon^2)^2 (f')^2}}. \quad (\text{E.18})$$

We can lower the order of the equation by defining $g(f) = f'$:

$$\frac{(1 + \epsilon^2 + \sqrt{4\epsilon^2 + (1 - \epsilon^2)^2 g^2})g'g}{(1 - g^2)\sqrt{4\epsilon^2 + (1 - \epsilon^2)^2 g^2}} = -\frac{2}{f}. \quad (\text{E.19})$$

And the solution is

$$g^2 = \frac{\epsilon^4 + (1 - (c_1 f)^2)^2 - 2\epsilon^2(1 + (c_1 f)^2)}{(1 - \epsilon^2)^2}, \quad (\text{E.20})$$

where c_1 is some constant. By requiring $g(f(1/2) = f_0) = 0$, we arrive at

$$c_1 f_0 = 1 - \epsilon, \quad c_1 = \frac{1 - \epsilon}{f_0}. \quad (\text{E.21})$$

Having found g as a function of f , we can now solve for f as a function of t . Setting $g = f'$ leads to

$$\frac{1}{c_1} H(c_1 f, \epsilon) = \frac{t}{1 - \epsilon^2} + c_2, \quad (\text{E.22})$$

where

$$H(x, \epsilon) = \frac{(1 + \epsilon) \sqrt{1 - \left(\frac{x}{1-\epsilon}\right)^2} \sqrt{1 - \left(\frac{x}{1+\epsilon}\right)^2} F\left(\arcsin\left(\frac{x}{1+\epsilon}\right), \left(\frac{1+\epsilon}{1-\epsilon}\right)^2\right)}{\sqrt{\epsilon^4 + (1 - x^2)^2 - 2\epsilon^2(1 + x^2)}}, \quad (\text{E.23})$$

and $F(x, a)$ is the incomplete elliptic integral (we use the same conventions as Wolfram Mathematica). Taking the limit $x \rightarrow 1 - \epsilon$ we have

$$H(1 - \epsilon, \epsilon) = \frac{K\left[\left(\frac{1-\epsilon}{1+\epsilon}\right)^2\right]}{1 + \epsilon}, \quad (\text{E.24})$$

where K is the complete elliptic integral.

We can use this expression to find c_1 and the value of the function at the maximum ($t = 1/2$)

$$2(1 - \epsilon)K\left[\left(\frac{1-\epsilon}{1+\epsilon}\right)^2\right] = c_1, \quad f_0 = \frac{1}{2K\left[\left(\frac{1-\epsilon}{1+\epsilon}\right)^2\right]}. \quad (\text{E.25})$$

As a consistency check we verify that for $\epsilon = 1$ we reproduce the old result $\lim_{\epsilon \rightarrow 1} f_0 = 1/\pi$ (the solution for a single branch was $\frac{\sin(\pi t)}{\pi}$).

The ‘‘on-shell’’ action can be rewritten as

$$I(\epsilon) = 2 \int_0^{f_0} \frac{df}{g(f)} (W(g(f), \epsilon) + 2 \log f), \quad (\text{E.26})$$

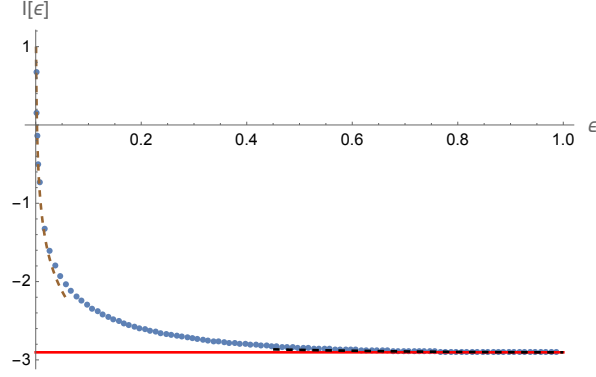


Figure 7. Numeric values of $I(\epsilon)$, shown in blue, vs the asymptotic value $I(1) = 2 \log \frac{2}{\pi e}$ for $\epsilon = 1$ (analytic value for the single branch), in red. Also, the asymptotic behavior $I(\epsilon) = 2 \log \frac{2}{\pi e} + (1 - \epsilon)^2/8$ for $\epsilon \rightarrow 1$ (E.48) (shown in dashed black), and the asymptotic behavior (E.40) for small ϵ (shown in dashed brown).

where f_0 and $g(f)$ are given by

$$f_0 = \frac{1}{2K \left[\left(\frac{1-\epsilon}{1+\epsilon} \right)^2 \right]}, \quad (\text{E.27})$$

$$g^2(f) = \frac{(f^2 - f_0^2)}{(1 + \epsilon)^2 f_0^4} \left[(1 - \epsilon)^2 f^2 - (1 + \epsilon)^2 f_0^2 \right]. \quad (\text{E.28})$$

Written explicitly, this integral is rather cumbersome and difficult to deal with. The numeric plot of I as a function of ϵ is shown in Fig. 7. The asymptotic behavior of the moments is

$$\boxed{\log \mu_{2n} \approx nI(\epsilon) + 2n \log(2\alpha n)}. \quad (\text{E.29})$$

If $\epsilon = 1$, $I(1) = 2 \log \frac{2}{\pi e}$ and $\log \mu_{2n} \approx 2n \log \frac{4\alpha n}{\pi e}$.

Leading asymptotic behavior of μ_{2n} for large n is fully determined by the location of the singularity of the correlation function $C(t)$ along the imaginary axis $t = i\tau^*$,

$$\log \mu_{2n} \approx 2n \log \frac{4\alpha_0 n}{\pi e}, \quad \alpha_0 = \pi/(2\tau^*). \quad (\text{E.30})$$

As we discussed in section 2.2, in field theory, symmetrically ordered correlation function (2.6) always has the singularity at $\tau^* = \beta/2$, and $\alpha_0 = \pi/\beta$. In the scenario of two slopes, we can express $\alpha_{\text{odd}}, \alpha_{\text{even}}$ (4.8) in terms of α_0 and ϵ

$$\frac{\alpha_{\text{odd}}}{\alpha_0} = \frac{2e^{-I(\epsilon)/2}}{\pi e} \frac{1}{\sqrt{\epsilon}}, \quad (\text{E.31})$$

$$\frac{\alpha_{\text{even}}}{\alpha_0} = \frac{2e^{-I(\epsilon)/2}}{\pi e} \sqrt{\epsilon}. \quad (\text{E.32})$$

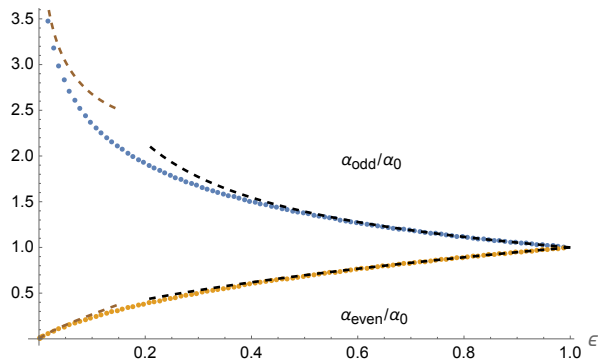


Figure 8. Ratio of $\alpha_{\text{odd}}/\alpha_0$ (blue) and $\alpha_{\text{even}}/\alpha_0$ (orange) as a function of ϵ , superimposed with the asymptotic behavior (E.50,E.51) for $\epsilon \rightarrow 1$ (dashed black), and (E.43,E.44) for $\epsilon \rightarrow 0$ (dashed brown).

In particular, plotting $\alpha_{\text{odd}}/\alpha_0$ and $\alpha_{\text{even}}/\alpha_0$ numerically, as a function of ϵ , see Fig. 8, we find that

$$\alpha_{\text{odd}} \geq \alpha_0 \geq \alpha_{\text{even}} \quad (\text{E.33})$$

always holds.

We remind the reader that, strictly speaking, α_{odd} and α_{even} are defined as slopes of faster and slower growing linear branches correspondingly, with no regard to whether corresponding index n is even or odd. In other words, the choice $\epsilon \leq 1$ introduced toward the end of section E.1 implies that by our definition $\alpha_{\text{odd}} \geq \alpha_{\text{even}}$.

As discussed in the main text, when $C(t) \rightarrow 0$ for $t \rightarrow \infty$, two slopes are only possible if the slope of the odd branch is larger than the slope of the even branch, consistent with (E.33). It is also conceivable (although no examples are known) that when $C(t)$ asymptotes to a non-zero constant, b_n might split into two linearly growing branches (for even and odd n), with $\alpha_{\text{odd}} \leq \alpha_{\text{even}}$. In this case (E.33) will read $\alpha_{\text{odd}} \leq \alpha_0 \leq \alpha_{\text{even}}$.

E.3 Small ϵ expansion

In this subsection, we continue discussing the case of two linear branches with different slopes and will determine the small ϵ behavior of $I(\epsilon)$. First of all, since we know the exact value of $f(1/2)$ we can find the limit

$$f(1/2) = f_0 \approx \frac{1}{|\log \epsilon|}. \quad (\text{E.34})$$

Next, at small ϵ (E.20) simplifies to

$$f'(t) = 1 - (f(t)/f_0)^2, \quad (\text{E.35})$$

which is solved by $f(t) = f_0 \tanh(t/f_0)$. While this solution seems to not be symmetric under $t \rightarrow 1 - t$, it should be thought of as only applicable at $t < 1/2$ and defined by symmetry for $t > 1/2$. This function is essentially constant for $t \gg \frac{1}{|\log \epsilon|}$ and, thus, stitching it with a different function at $t = 1/2$ is appropriate.

Now, we expand $W(f', \epsilon)$.

$$W(f', \epsilon) \approx S(f') + |\log \epsilon|(1 - f'), \quad (\text{E.36})$$

$$I(\epsilon) = 2 \int_0^{1/2} dt (S(f') - |\log \epsilon| f') + |\log \epsilon| + 4 \int_0^{1/2} dt \log(f), \quad (\text{E.37})$$

$$\int_0^\infty (S(f') - |\log \epsilon| f') \approx \frac{\pi^2/4 - \log(4)}{|\log \epsilon|} - 1, \quad (\text{E.38})$$

$$\int_0^{1/2} dt \log(f) \approx -\frac{\pi^2}{8} \frac{1}{|\log \epsilon|} - \frac{1}{2} \log |\log \epsilon|. \quad (\text{E.39})$$

Collecting all the terms together,

$$I(\epsilon) = |\log \epsilon| - 2 \log |\log \epsilon| - 2 - \frac{2 \log 4}{|\log \epsilon|} + \dots \quad (\text{E.40})$$

Since the leading behavior of moments is

$$\log \mu_{2n} \approx nI(\epsilon) + 2n \log(2\alpha n), \quad (\text{E.41})$$

this means corresponding correlation function $C(t)$ will have a singularity at

$$it = \tau^* \approx -\frac{\epsilon^{1/2} \log \epsilon}{\alpha} \quad (\text{E.42})$$

and

$$\frac{\alpha_{\text{odd}}}{\alpha_0} = -\frac{2}{\pi} \log \epsilon e^{-\log(4)/\log \epsilon}, \quad (\text{E.43})$$

$$\frac{\alpha_{\text{even}}}{\alpha_0} = -\frac{2}{\pi} \epsilon \log \epsilon e^{-\log(4)/\log \epsilon}. \quad (\text{E.44})$$

We can check this result by comparing with the small radius expansion (4.4), when, at leading order

$$\alpha = \frac{2\pi}{\beta R} e^{-\frac{\pi}{4R}} \quad \epsilon = 4e^{-\frac{\pi}{2R}}, \quad R \rightarrow 0, \quad (\text{E.45})$$

and we restored β -dependence. Plugging this into (E.42) yields $\tau^* = \beta/2$, which is the universal result for field theory and readily follows from (4.1). In other words, small radius expansion (4.4) is in agreement with (E.42).

E.4 $1 - \epsilon$ expansion

Let us define $\epsilon = 1 - \delta$. We can expand

$$f_0 \approx \frac{1}{\pi} - \frac{\delta^2}{16\pi}. \quad (\text{E.46})$$

The correction to the action is

$$\delta S = \frac{\delta^2}{4} \int_0^1 dt (1 - (f')^2). \quad (\text{E.47})$$

Since the variation of the action vanishes on the saddle point solution the contribution coming from the change in the saddle point will be of order δ^4 . Thus, to leading order we only need to evaluate the value of (E.47),

$$\delta S = \frac{\delta^2}{8}. \quad (\text{E.48})$$

Finally,

$$\log \mu_{2n} = 2n \left(\log \frac{4\alpha n}{\pi e} + \frac{\delta^2}{16} \right) + O(\delta^4). \quad (\text{E.49})$$

This means, for $\delta \ll 1$, the correlation function will have a singularity at $it = \tau^* = \pi/(2\alpha)e^{-\delta^2/16}$. For field theory, in full generality we expect this to be equal to $\tau^* = \beta/2$, and hence $\alpha = \pi/\beta e^{-\delta^2/16}$. This of course reduces to standard result $b_n \sim \frac{\pi}{\beta}n$ when there is one linear slope, as in conformal field theories in flat space considered in [4]. For the “two slopes behavior” (4.8) we find in full generality ,

$$\alpha_{\text{odd}} = \alpha_0(1 - \delta)^{-1/2}e^{-\delta^2/16}, \quad (\text{E.50})$$

$$\alpha_{\text{even}} = \alpha_0(1 - \delta)^{+1/2}e^{-\delta^2/16}, \quad (\text{E.51})$$

when $\delta \ll 1$, i.e. when $\alpha_{\text{even}}/\alpha_{\text{odd}}$ is very close to one. It would be interesting to compare this prediction with the large R limit of b_n for (4.1).

E.5 Persistent staggering behavior

In section 3 we saw that for massive theories Lanczos coefficients exhibit “persistent staggering” behavior (3.1). It also can be described via the general formalism developed in section E.1 above. We assume $b_{\text{even}} = \alpha n + c_e, b_{\text{odd}} = \alpha n + c_o$ and in this case $\epsilon = 1 + c/n + \dots$ where $c = c_o - c_e$ is a constant. For $c = 0$ the problem reduces to

the original single-slope, no intercept problem, which is solved by $f(t) = \frac{\sin(\pi t)}{\pi}$. For non-zero c we treat $\frac{c}{n}$ as a perturbation and obtain

$$W(f', \epsilon) = (\text{c=0 part}) + c^2 \frac{\sin(\pi t)^2}{4n^2} + \dots \quad (\text{E.52})$$

Upon integration, the leading-order correction is $\frac{c^2}{8n}$, while the $c = 0$ result with $c_e = c_o \neq 0$ was calculated in [4],

$$\log \mu_{2n} = 2n \log \frac{4\alpha n}{\pi e} + \frac{c_e + c_o}{\alpha} \log(2n) + \dots \quad (\text{E.53})$$

It is clear that $\frac{c^2}{8n}$ is subleading and does not affect the singularity behavior of $C(t) \sim (t - i\tau^*)^{-2\Delta}$, which follows from (E.53),

$$\tau^* = \frac{\pi}{2\alpha}, \quad 2\Delta - 1 = \frac{c_e + c_o}{\alpha}. \quad (\text{E.54})$$

References

- [1] D. E. Parker, X. Cao, A. Avdoshkin, T. Scaffidi and E. Altman, *A universal operator growth hypothesis*, *Physical Review X* **9** (2019) .
- [2] T. A. Elsayed, B. Hess and B. V. Fine, *Signatures of chaos in time series generated by many-spin systems at high temperatures*, *Physical Review E* **90** (2014) 022910.
- [3] A. Avdoshkin and A. Dymarsky, *Euclidean operator growth and quantum chaos*, *Physical Review Research* **2** (2020) .
- [4] A. Dymarsky and M. Smolkin, *Krylov complexity in conformal field theory*, *Phys. Rev. D* **104** (2021) L081702 [2104.09514].
- [5] B. Bhattacharjee, X. Cao, P. Nandy and T. Pathak, *Krylov complexity in saddle-dominated scrambling*, *Journal of High Energy Physics* **2022** (2022) .
- [6] J. Maldacena, S. H. Shenker and D. Stanford, *A bound on chaos*, *Journal of High Energy Physics* **2016** (2016) 106.
- [7] Y. Gu, A. Kitaev and P. Zhang, *A two-way approach to out-of-time-order correlators*, *Journal of High Energy Physics* **2022** (2022) .
- [8] L. Susskind, *Computational Complexity and Black Hole Horizons*, *Fortsch. Phys.* **64** (2016) 24 [1403.5695].
- [9] A. R. Brown, D. A. Roberts, L. Susskind, B. Swingle and Y. Zhao, *Holographic Complexity Equals Bulk Action?*, *Phys. Rev. Lett.* **116** (2016) 191301 [1509.07876].
- [10] A. R. Brown, D. A. Roberts, L. Susskind, B. Swingle and Y. Zhao, *Complexity, action, and black holes*, *Phys. Rev. D* **93** (2016) 086006 [1512.04993].

- [11] O. Ben-Ami and D. Carmi, *On Volumes of Subregions in Holography and Complexity*, *JHEP* **11** (2016) 129 [[1609.02514](#)].
- [12] S. Chapman, H. Marrochio and R. C. Myers, *Complexity of Formation in Holography*, *JHEP* **01** (2017) 062 [[1610.08063](#)].
- [13] D. Carmi, S. Chapman, H. Marrochio, R. C. Myers and S. Sugishita, *On the Time Dependence of Holographic Complexity*, *JHEP* **11** (2017) 188 [[1709.10184](#)].
- [14] A. Belin, R. C. Myers, S.-M. Ruan, G. Sárosi and A. J. Speranza, *Does Complexity Equal Anything?*, *Phys. Rev. Lett.* **128** (2022) 081602 [[2111.02429](#)].
- [15] S.-K. Jian, B. Swingle and Z.-Y. Xian, *Complexity growth of operators in the SYK model and in JT gravity*, *Journal of High Energy Physics* **2021** (2021) .
- [16] V. Balasubramanian, P. Caputa, J. Magan and Q. Wu, *Quantum chaos and the complexity of spread of states*, 2022. 10.48550/ARXIV.2202.06957.
- [17] A. Dymarsky and A. Gorsky, *Quantum chaos as delocalization in krylov space*, *Physical Review B* **102** (2020) 085137.
- [18] D. J. Yates, A. G. Abanov and A. Mitra, *Lifetime of almost strong edge-mode operators in one-dimensional, interacting, symmetry protected topological phases*, *Phys. Rev. Lett.* **124** (2020) 206803.
- [19] D. J. Yates, A. G. Abanov and A. Mitra, *Dynamics of almost strong edge modes in spin chains away from integrability*, *Physical Review B* **102** (2020) .
- [20] D. J. Yates, A. G. Abanov and A. Mitra, *Long-lived period-doubled edge modes of interacting and disorder-free Floquet spin chains*, [2105.13766](#).
- [21] D. J. Yates and A. Mitra, *Strong and almost strong modes of Floquet spin chains in Krylov subspaces*, *Phys. Rev. B* **104** (2021) 195121 [[2105.13246](#)].
- [22] J. D. Noh, *Operator growth in the transverse-field ising spin chain with integrability-breaking longitudinal field*, *Physical Review E* **104** (2021) .
- [23] F. B. Trigueros and C.-J. Lin, *Krylov complexity of many-body localization: Operator localization in Krylov basis*, [2112.04722](#).
- [24] C. Liu, H. Tang and H. Zhai, *Krylov complexity in open quantum systems*, 2022. 10.48550/ARXIV.2207.13603.
- [25] Z.-Y. Fan, *Universal relation for operator complexity*, *Physical Review A* **105** (2022) .
- [26] A. Kar, L. Lamprou, M. Rozali and J. Sully, *Random matrix theory for complexity growth and black hole interiors*, *Journal of High Energy Physics* **2022** (2022) .
- [27] J. L. F. Barbón, E. Rabinovici, R. Shir and R. Sinha, *On The Evolution Of Operator Complexity Beyond Scrambling*, *JHEP* **10** (2019) 264 [[1907.05393](#)].

- [28] E. Rabinovici, A. Sánchez-Garrido, R. Shir and J. Sonner, *Operator complexity: a journey to the edge of krylov space*, *Journal of High Energy Physics* **2021** (2021) .
- [29] E. Rabinovici, A. Sánchez-Garrido, R. Shir and J. Sonner, *Krylov localization and suppression of complexity*, *Journal of High Energy Physics* **2022** (2022) .
- [30] E. Rabinovici, A. Sánchez-Garrido, R. Shir and J. Sonner, *Krylov complexity from integrability to chaos*, *Journal of High Energy Physics* **2022** (2022) .
- [31] P. Caputa, J. M. Magan and D. Patramanis, *Geometry of krylov complexity*, *Physical Review Research* **4** (2022) 013041.
- [32] P. Caputa and S. Datta, *Operator growth in 2d CFT*, *Journal of High Energy Physics* **2021** (2021) .
- [33] P. Caputa and S. Liu, *Quantum complexity and topological phases of matter*, 2022. 10.48550/ARXIV.2205.05688.
- [34] R. Heveling, J. Wang and J. Gemmer, *Numerically probing the universal operator growth hypothesis*, *Phys. Rev. E* **106** (2022) 014152.
- [35] K. Adhikari and S. Choudhury, *cosmological krylov complexity*, 2022. 10.48550/ARXIV.2203.14330.
- [36] K. Adhikari, S. Choudhury and A. Roy, *krylov complexity in Quantum field theory*, 2022. 10.48550/ARXIV.2204.02250.
- [37] W. Mück and Y. Yang, *Krylov complexity and orthogonal polynomials*, 2022. 10.48550/ARXIV.2205.12815.
- [38] A. Bhattacharya, P. Nandy, P. P. Nath and H. Sahu, *Operator growth and krylov construction in dissipative open quantum systems*, 2022. 10.48550/ARXIV.2207.05347.
- [39] N. Hörnedal, N. Carabba, A. S. Matsoukas-Roubeas and A. del Campo, *Ultimate speed limits to the growth of operator complexity*, *Communications Physics* **5** (2022) .
- [40] S. Guo, *Operator growth in su(2) yang-mills theory*, 2022. 10.48550/ARXIV.2208.13362.
- [41] M. Afrasiar, J. K. Basak, B. Dey, K. Pal and K. Pal, *Time evolution of spread complexity in quenched lipkin-meshkov-glick model*, 2022. 10.48550/ARXIV.2208.10520.
- [42] V. Balasubramanian, J. M. Magan and Q. Wu, *A tale of two hungarians: Tridiagonalizing random matrices*, 2022. 10.48550/ARXIV.2208.08452.
- [43] S. Baek, *Krylov complexity in inverted harmonic oscillator*, 2022. 10.48550/ARXIV.2210.06815.
- [44] B. Bhattacharjee, X. Cao, P. Nandy and T. Pathak, *An operator growth hypothesis for open quantum systems*, **2212.06180**.
- [45] S. He, P. H. C. Lau, Z.-Y. Xian and L. Zhao, *Quantum chaos, scrambling and operator growth in $T\bar{T}$ deformed SYK models*, *JHEP* **12** (2022) 070 [[2209.14936](#)].

- [46] M. Alishahiha and S. Banerjee, *A universal approach to Krylov State and Operator complexities*, [2212.10583](#).
- [47] B. Bhattacharjee, S. Sur and P. Nandy, *Probing quantum scars and weak ergodicity breaking through quantum complexity*, *Phys. Rev. B* **106** (2022) 205150 [[2208.05503](#)].
- [48] B. Bhattacharjee, P. Nandy and T. Pathak, *Krylov complexity in large- q and double-scaled SYK model*, [2210.02474](#).
- [49] H. A. Camargo, V. Jahnke, K.-Y. Kim and M. Nishida, *Krylov complexity in free and interacting scalar field theories with bounded power spectrum*, *JHEP* **05** (2023) 226 [[2212.14702](#)].
- [50] S. Khetrapal, *Chaos and operator growth in 2d CFT*, [2210.15860](#).
- [51] H. Araki, *Gibbs states of a one dimensional quantum lattice*, *Communications in Mathematical Physics* **14** (1969) 120.
- [52] V. Viswanath and G. Müller, *The Recursion Method: Application to Many-Body Dynamics*, vol. 23. Springer Science & Business Media, 2008.
- [53] L. F. Alday, M. Kologlu and A. Zhiboedov, *Holographic correlators at finite temperature*, *JHEP* **06** (2021) 082 [[2009.10062](#)].
- [54] E. Keski-Vakkuri, *Bulk and boundary dynamics in BTZ black holes*, *Phys. Rev. D* **59** (1999) 104001 [[hep-th/9808037](#)].
- [55] J. M. Maldacena, *Eternal black holes in anti-de Sitter*, *JHEP* **04** (2003) 021 [[hep-th/0106112](#)].
- [56] T. Anous and J. Sonner, *Phases of scrambling in eigenstates*, *SciPost Phys.* **7** (2019) 003 [[1903.03143](#)].
- [57] T. LeBlond, K. Mallayya, L. Vidmar and M. Rigol, *Entanglement and matrix elements of observables in interacting integrable systems*, *Phys. Rev. E* **100** (2019) 062134.
- [58] X. Cao, *A statistical mechanism for operator growth*, *Journal of Physics A: Mathematical and Theoretical* **54** (2021) 144001.
- [59] G. Bouch, *The expected perimeter in eden and related growth processes*, *Journal of Mathematical Physics* **56** (2015) 123302.
- [60] P. Caputa and J. M. Magan, *Quantum computation as gravity*, *Physical review letters* **122** (2019) 231302.
- [61] D. V. Vassilevich, *Heat kernel expansion: User's manual*, *Phys. Rept.* **388** (2003) 279 [[hep-th/0306138](#)].
- [62] R. Camporesi and A. Higuchi, *Spectral functions and zeta functions in hyperbolic spaces*, *J. Math. Phys.* **35** (1994) 4217.
- [63] T. Niemeijer, *Some exact calculations on a chain of spins 1/2*, *Physica* **36** (1967) 377.